PNAS RESEARCH ARTICLE | DEVELOPMENTAL BIOLOGY

CDYL reinforces male gonadal sex determination through epigenetically repressing *Wnt4* transcription in mice

Naoki Okashita[a], Ryo Maeda[a], and Makoto Tachibana[a,1]

Edited by Blanche Capel, Duke University Hospital, Durham, NC; received December 19, 2022; accepted April 1, 2023 by Editorial Board Member Denis Duboule

In mammals, male and female gonads initially develop from bipotential progenitor cells, which can differentiate into either testicular or ovarian cells. The decision to adopt a testicular or ovarian fate relies on robust genetic forces, i.e., activation of the testis-determining gene *Sry*, as well as a delicate balance of expression levels for pro-testis and pro-ovary factors. Recently, epigenetic regulation has been found to be a key element in activation of *Sry*. Nevertheless, the mechanism by which epigenetic regulation controls the expression balance of pro-testis and pro-ovary factors remains unclear. Chromodomain Y-like protein (CDYL) is a reader protein for repressive histone H3 methylation marks. We found that a subpopulation of *Cdyl*-deficient mice exhibited XY sex reversal. Gene expression analysis revealed that the testis-promoting gene *Sox9* was downregulated in XY *Cdyl*-deficient gonads during the sex determination period without affecting *Sry* expression. Instead, we found that the ovary-promoting gene *Wnt4* was derepressed in XY *Cdyl*-deficient gonads prior to and during the sex-determination period. *Wnt4* heterozygous deficiency restored *SOX9* expression in *Cdyl*-deficient XY gonads, indicating that derepressed *Wnt4* is a cause of the repression of *Sox9*. We found that CDYL directly bound to the *Wnt4* promoter and maintained its H3K27me3 levels during the sex-determination period. These findings indicate that CDYL reinforces male gonadal sex determination by repressing the ovary-promoting pathway in mice.

CDYL | WNT4 | gonadal sex determination | H3K27me3

Significance

Sex determination is the fate decision by which bipotential gonads develop into either testes or ovaries. Sex determination relies on a balance of expression levels of testis- and ovary-promoting genes; however, the mechanisms that tune this balance are not fully understood. We found that the epigenetic regulator, CDYL (Chromodomain Y-like protein), is involved in this process. CDYL indirectly reinforces the expression of the testis-promoting gene *Sox9* by directly binding to and repressing the ovary-promoting gene *Wnt4*.

Eukaryotic genetic information is stored in chromatin, which is fundamentally composed of genomic DNA and histones. Structural changes in chromatin are closely related to transcriptional activation or suppression. Covalent modifications of DNA and histones in chromatin play indispensable roles in transcriptional regulation. A variety of chemical tags are added to DNA and histones, imparting distinct transcriptional competence to chromatin. A large number of enzymes contributing to these processes are categorized as "writers" which introduce chemical tags on DNA/histones and "erasers" which remove the tags (1). In addition to writers and erasers, "reader" proteins play a key role in gene regulation in chromatin environment (1). Namely, covalent modifications of chromatin are recognized by the corresponding readers through their specialized domains and then translated into specific biological outputs, including transcriptional activation or suppression. Currently, more than 10 types of reader modules have been identified (2).

Sex determination refers to the developmental decision that directs sexually undifferentiated embryonic gonads to differentiate into either testes or ovaries. In mammals, the testis-promoting pathway is activated by the expression of the Y-linked testis-determining gene *SRY*/*Sry*, which promotes the differentiation of sexually undifferentiated gonadal somatic cells into testicular supporting cells (Sertoli cells). *Sry* in mice is the most intensively studied model for mammalian sex determination. *Sry* expression is controlled in a spatially and temporally stringent manner; it is expressed only in a limited population of embryonic gonadal somatic cells and only from embryonic day (E) 10.5 to 12.5. SRY activates the transcription of *Sox9*, which is essential for Sertoli cell differentiation, by directly binding to its enhancer region (3). In the absence of *Sry*, *Sox9* transcription is not activated but ovary-promoting genes are expressed. Importantly, testis- and ovary-promoting mechanisms are mutually antagonistic, with each pathway repressing the other (4). For example, ovary-promoting genes *Wnt4*, *Rspo1*, and *Foxl2* are involved in the repression of *Sox9*, and mutations in these genes lead to the activation of the testis-promoting pathway through the derepression of *Sox9* (4).

Recent genetic studies in mice have revealed that modifications of histones and DNA substantially contribute to mammalian sex determination. Di- or trimethylated H3K9 (H3K9me2/3) is a hallmark of transcriptionally suppressed chromatin. We previously showed that the H3K9 demethylase JMJD1A activates *Sry* transcription by removing H3K9me2

Author affiliations: [a]Laboratory of Epigenome Dynamics, Graduate School of Frontier Biosciences, Osaka University, Suita, Osaka 565-0871, Japan

Author contributions: N.O. and M.T. designed research; N.O. performed research; N.O. contributed new reagents/analytic tools; N.O. and R.M. analyzed data; and N.O. and M.T. wrote the paper.

The authors declare no competing interest.

This article is a PNAS Direct Submission. B.C. is a guest editor invited by the Editorial Board.

[1]To whom correspondence may be addressed. Email: tachiban@fbs.osaka-u.ac.jp.

This article contains supporting information online at https://www.pnas.org/lookup/suppl/doi:10.1073/pnas.2221499120/-/DCSupplemental.

Published May 8, 2023.

during male gonadal sex determination; loss of JMJD1A in mice led to increased H3K9me2 at the *Sry* locus and diminished *Sry* expression, resulting in XY sex reversal (5). We further demonstrated that H3K9 methyltransferase GLP/G9a functions in opposition to JMJD1A-mediated *Sry* activation; a heterozygous *GLP* mutation rescued the sex-reversal phenotype of *Jmjd1a*-deficient mice by reducing H3K9me2 at the *Sry* locus and increasing *Sry* expression (6). These studies indicated that the G9a/GLP complex and JMJD1A are the writer and eraser proteins responsible for tuning H3K9me2 at the *Sry* locus, respectively. Histone acetylation is involved in transcriptional activation. Loss of histone acetyl transferases, CBP and p300, led to decreased H3K27 acetylation at the *Sry* locus and reduced *Sry* expression, resulting in complete XY sex reversal (7). H3K27me3 is involved in the transcriptional suppression of developmentally regulated genes. A previous study showed that the loss of a chromodomain-containing protein, CBX2, led to male-to-female sex reversal (8). CBX2 suppresses the ovary-promoting gene *Lef1* in XY gonads during male sex determination. Derepressed *Lef1* in *Cbx2*-deficient gonads induces the transcriptional suppression of *Sry* (9). In addition to histone modifications, active DNA demethylation catalyzed by 5-methylcytosine oxidase TET2 is involved in the positive regulation of *Sry* (10).

We have previously identified the H3K9me2 writer and eraser proteins for the *Sry* locus, and here aimed to identify the H3K9me2 reader protein for the *Sry* locus. Chromodomain Y-like protein (CDYL), which was cloned in 1999, contains an amino-terminal canonical chromodomain and a carboxy-terminal enoyl-coenzyme A hydratase/isomerase catalytic domain (11). CDYL was initially reported as a regulator of spermatogenesis (12). Recently, it was shown that CDYL plays a key role in controlling neuronal intrinsic excitability (13). We predicted that CDYL might be an H3K9me2 reader protein for the *Sry* locus and suppress its expression for several reasons. First, the chromodomain of CDYL binds to suppressive methylation marks of histone H3, including H3K9me2 and H3K27me3 (14). Second, CDYL physiologically interacts with the H3K9 methyltransferase GLP/G9a, which is the writer for H3K9me2 at the *Sry* locus (15, 16). Third, CDYL is involved in several co-repressor complexes, such as CtBP (17) and the REST complex (18). Finally, CDYL epigenetically represses transcription of the target genes (19, 20). To test this hypothesis, we introduced a heterozygous mutation of *Cdyl* into the *Jmjd1a*-deficient background and then analyzed whether *Cdyl* mutation could rescue the XY sex-reversal phenotype of *Jmjd1a*-deficient mice, similar to the case of *GLP* heterozygous mutation (6). Unexpectedly, *Cdyl* heterozygous mutation further enhanced the XY sex reversal phenotype of *Jmjd1a*-deficient mice, indicating that CDYL positively regulates male development. In this study, we revealed the mode of action of CDYL in male gonadal sex determination.

Results

***Cdyl* Heterozygous Deficiency Enhances XY Sex Reversal Phenotype of *Jmjd1a*-Deficient Mice.** XY *Jmjd1a*-deficient ($Jmjd1a^{\Delta/\Delta}$) mice exhibit partial sex reversal phenotype (5) and hence can serve as a model to study how mutations of additional genes may aggravate or eliminate this phenotype (Fig. 1*A*). For example, mutation of *GLP*, which encodes an H3K9 methyltransferase, suppressed XY sex reversal in $Jmjd1a^{\Delta/\Delta}$ mice (6), revealing that GLP is a negative regulator of male sex development. In contrast, *Tet2* mutation enhanced XY sex reversal in $Jmjd1a^{\Delta/\Delta}$ mice (10), revealing that TET2 is a positive regulator of male sex development. To evaluate the contribution of CDYL to sex development, we established mouse lines carrying the *Cdyl* mutant allele ($Cdyl^{\Delta}$) using the CRISPR/Cas9 system (*SI Appendix*, Fig. S1*A*). We found that most $Cdyl^{\Delta/\Delta}$ mice died shortly after birth, and only a subpopulation survived to week 8 (*SI Appendix*, Fig. S1*C*), which was consistent with a previous study (21). After sequentially crossing $Cdyl^{\Delta}$ into the $Jmjd1a^{\Delta}$ background, we generated XY $Cdyl^{\Delta/+}$; $Jmjd1a^{\Delta/\Delta}$ mice and compared their sex development phenotypes with those of XY $Cdyl^{+/+}$; $Jmjd1a^{\Delta/\Delta}$ littermates. Previous studies have demonstrated that CDYL represses transcription by interacting with GLP/G9a and H3K9me2 (15, 16); therefore, we speculated that *Cdyl* mutation might rescue the XY sex reversal phenotype of $Jmjd1a^{\Delta/\Delta}$ mice. However, contrary to our expectations, $Cdyl^{\Delta}$ allele dramatically enhanced XY sex reversal in $Jmjd1a^{\Delta/\Delta}$ mice (Fig. 1*B*). Consistent with our previous results (5), the subpopulation of XY $Jmjd1a^{\Delta/\Delta}$ mice exhibited sex reversal; of the 35 XY $Cdyl^{+/+}$; $Jmjd1a^{\Delta/\Delta}$ mice, 25 (71%) were sex-reversed completely or partially, and the remaining 10 (29%) developed as male. In contrast, of the 38 XY $Cdyl^{\Delta/+}$; $Jmjd1a^{\Delta/\Delta}$ mice, almost all animals (37, 97%) exhibited complete sex reversal.

To address how *Cdyl* mutation influences embryonic gonadal sex development just after sex determination, we evaluated gonadal sex differentiation of E13.5 embryos using antibodies against the testicular somatic cell marker SOX9 and the ovarian somatic cell marker FOXL2 (Fig. 1*C*). XY $Cdyl^{\Delta/+}$; $Jmjd1a^{\Delta/+}$ gonads (male control) contained only SOX9-positive (SOX9+) cells that formed tubule-like structures. In contrast, the XX $Cdyl^{\Delta/+}$; $Jmjd1a^{\Delta/+}$ gonads (female control) contained only FOXL2+ cells. XY $Cdyl^{+/+}$; $Jmjd1a^{\Delta/\Delta}$ gonads were ovotestes containing both SOX9+ and FOXL2+ cells. Importantly, *Cdyl* mutation led to a remarkable increase in the ratio of FOXL2+ cells in XY $Jmjd1a^{\Delta/\Delta}$ gonads; the ratio of FOXL2+ cells to the sum of FOXL2+ cells and SOX9+ cells was approximately 60% in XY $Cdyl^{+/+}$; $Jmjd1a^{\Delta/\Delta}$ gonads, whereas it was elevated to approximately 90% in XY $Cdyl^{\Delta/+}$; $Jmjd1a^{\Delta/\Delta}$ gonads. These data indicated that CDYL positively regulates male embryonic gonadal sex development.

A Subpopulation of *Cdyl*-Deficient Mice Exhibits XY Sex Reversal. We examined whether *Cdyl* deficiency induces XY sex reversal in the *Jmjd1a* wild-type background. We examined the external and internal genitalia of the postnatal and sexually mature XY $Cdyl^{\Delta/\Delta}$ mice. None of the 124 XY $Cdyl^{\Delta/+}$ mice exhibited sex reversal. However, of the 62 XY $Cdyl^{\Delta/\Delta}$ mice, 6 (10%) carried female-type genitalia (Fig. 2*A*), indicating that a subpopulation of $Cdyl^{\Delta/\Delta}$ mice exhibited XY sex reversal. Next, we analyzed gonadal sex development in E13.5 XY $Cdyl^{\Delta/\Delta}$ embryos (Fig. 2*B*). We found that all XY $Cdyl^{\Delta/\Delta}$ embryos examined carried ovotestes containing 40% population of FOXL2+ cells and 60% population of SOX9+ cells on average (Fig. 2*B*). In contrast to the abnormal testis development of XY $Cdyl^{\Delta/\Delta}$ gonads, XX $Cdyl^{\Delta/\Delta}$ gonads appeared to differentiate into normal ovaries (*SI Appendix*, Fig. S2*A*). Collectively, these data confirm that CDYL is a positive regulator of the testis-promoting pathway.

CDYL and its related protein CDYL2 (22) have similar molecular functions (23). To evaluate whether *Cdyl2* deficiency affects male gonadal sex development, we established mouse lines carrying *Cdyl2* mutant allele ($Cdyl2^{\Delta}$) using the CRISPR/Cas9 system (*SI Appendix*, Fig. S1*B*). By crossing $Cdyl2^{\Delta/+}$ parents, we obtained $Cdyl2^{\Delta/\Delta}$ offspring and evaluated their sex development. Of the 78 postnatal XY $Cdyl2^{\Delta/\Delta}$ mice, none underwent sex reversal (*SI Appendix*, Fig. S2*B*). We found that most gonadal somatic cells differentiated into SOX9+ cells and a few differentiated into FOXL2+ cells in E13.5 XY $Cdyl2^{\Delta/\Delta}$ embryos (*SI Appendix*, Fig. S2*C*). Next, by sequentially crossing the $Cdyl2^{\Delta}$ allele with the $Cdyl^{\Delta}$ background, we obtained $Cdyl^{\Delta/\Delta}$; $Cdyl2^{\Delta/\Delta}$ mice and examined their phenotypes. The sex

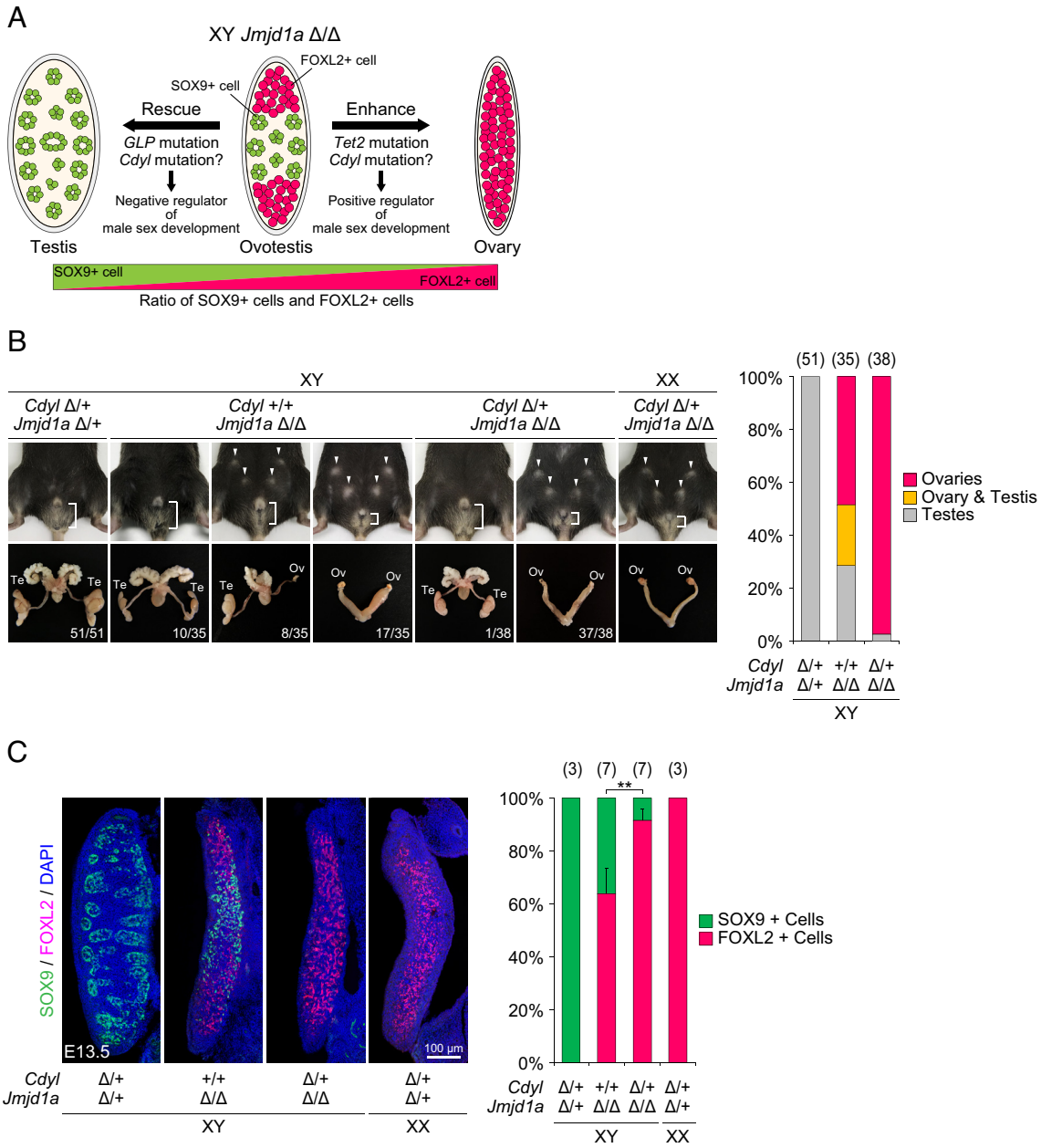

Fig. 1. *Cdyl* heterozygous deficiency enhances sex reversal of XY *Jmjd1a*-deficient mice. (*A*) Schematic illustration to identify the factors involved in mouse gonadal sex development using XY *Jmjd1a*$^{\Delta/\Delta}$ mice. XY *Jmjd1a*$^{\Delta/\Delta}$ mice have ovotestis containing both SOX9+ cells and FOXL2+ cells (5). We introduced a mutant allele of gene of interest into *Jmjd1a*$^{\Delta/\Delta}$ background and then examined gonadal sex development of the corresponding XY mice. For example, *GLP* mutation had rescued the ovotestis phenotype in XY *Jmjd1a*$^{\Delta/\Delta}$ gonads, indicating that GLP is a negative regulator of the testis-promoting pathway (6). Conversely, *Tet2* mutation had enhanced sex reversal in XY *Jmjd1a*$^{\Delta/\Delta}$ gonads, indicating that TET2 is a positive regulator of the testis-promoting pathway (10). (*B*) Comparative analysis of external genitalia (*Upper*) and internal genitalia (*Lower*) of 2 to 3-mo–old mice carrying *Cdyl*$^{\Delta}$ allele on the *Jmjd1a*$^{\Delta/\Delta}$ background. Arrowheads represent mammary glands. The distance between the anus and penis or vagina is indicated. Frequencies are presented in the lower right corner. Te, Testis; Ov, Ovary. Sex differentiation of internal genitalia of 2 to 3-mo–old mice of the indicated genotypes are summarized on the *Right*. Gray bar indicates mice carrying two testes. Yellow bar indicates mice carrying one testis and one ovary. Red bar indicates mice carrying two ovaries. The number of animals examined is shown above the bars. (*C*) Evaluation of gonadal sex differentiation of XY *Cdyl*$^{\Delta/+}$; *Jmjd1a*$^{\Delta/\Delta}$ embryos by immunofluorescence. E13.5 gonads of the indicated genotypes were co-stained with antibodies against testicular somatic cell marker SOX9 and ovarian somatic cell marker FOXL2. The ratio of SOX9+ to FOXL2+ cells is summarized on the *Right*. The green and red bars indicate SOX9+ and FOXL2+ cells, respectively. The number of embryos examined is shown above the bars. Data are presented as the mean ±SD, $^{**}P < 0.01$.

development phenotype of XY *Cdyl*$^{\Delta/\Delta}$; *Cdyl2*$^{\Delta/\Delta}$ was almost identical to that of XY *Cdyl*$^{\Delta/\Delta}$; *Cdyl2*$^{+/+}$ mice (*SI Appendix*, Fig. S2 *B* and *C*). These data indicated that CDYL2 has a limited contribution to male gonadal sex development. We previously established *Nr5a1-hCD271*-transgenic (tg) mice in which NR5A1+ gonadal somatic cells were tagged with a cell surface antigen, hCD271 (5, 24). Using this tg line, we isolated NR5A1-expressing cells from gonad-mesonephros pairs of XY embryos at the sex-determining period (E11.5) by magnetic-activated cell sorting (MACS), and then analyzed their mRNA expression (SRA: PRJNA557299) (10). We found that the expression levels of *Cdyl2* mRNA were only approximately 1/4 of those of *Cdyl* in E11.5 embryonic gonadal somatic cells (Fig. 2*C*), possibly explaining the limited effect of *Cdyl2* deficiency on male gonad development.

***Cdyl* Deficiency Reduces *Sox9* Expression Without Affecting *Sry* Expression in Gonadal Somatic Cells during the Sex Determination Period.** Next, we evaluated how CDYL contributes

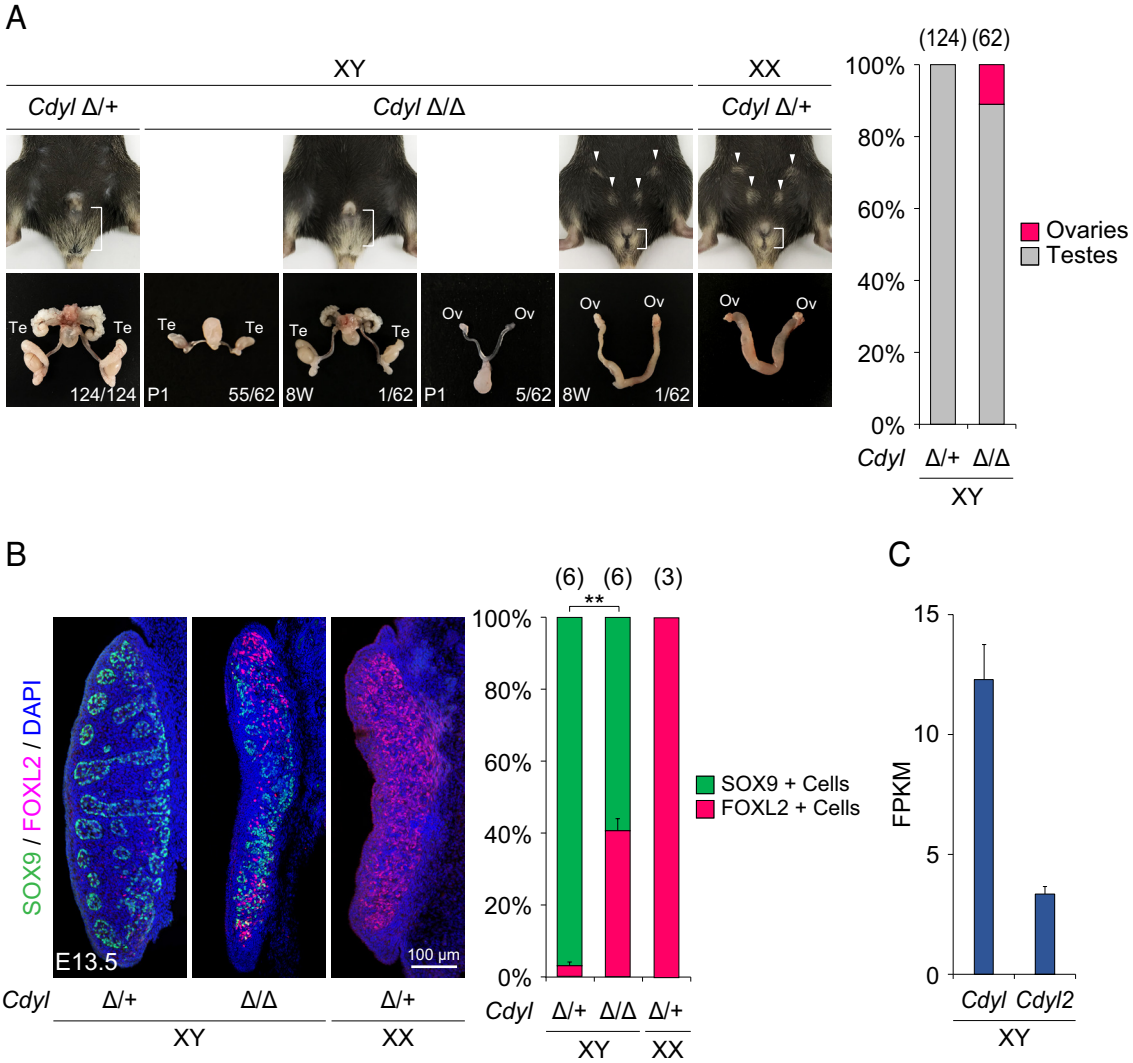

Fig. 2. A subpopulation of *Cdyl*-deficient mice exhibits XY sex reversal. (*A*) Comparative analysis of external genitalia (*Upper*) and internal genitalia (*Lower*) between XY *Cdyl*$^{\Delta/+}$ and *Cdyl*$^{\Delta/\Delta}$ mice at 1 d or 2 to 3 mo age. Internal genitalia of 1-d–old (P1) XY *Cdyl*$^{\Delta/\Delta}$ mice and external/internal genitalia of 2-mo–old (8W) XY *Cdyl*$^{\Delta/\Delta}$ mice are shown. Arrowheads represent mammary glands. The distance between the anus and penis or vagina is indicated. Frequencies are presented in the lower right corner. Te, Testis; Ov, Ovary. Sex differentiation of internal genitalia of 1-d to 3-mo–old mice are summarized on the *Right*. The gray and red bars indicate mice carrying two testes and those carrying two ovaries, respectively. The number of animals examined is shown above the bars. The majority of *Cdyl*$^{\Delta/\Delta}$ mice were analyzed within 2 d after birth. (*B*) Evaluation of gonadal sex differentiation of *Cdyl*$^{\Delta/\Delta}$ embryos by immunofluorescence. E13.5 gonads of the indicated genotypes were co-stained with antibodies against SOX9 and FOXL2. The ratio of SOX9+ to FOXL2+ cells is summarized on the *Right*. The green and red bars indicate SOX9+ and FOXL2+ cells, respectively. The number of embryos examined is shown above the bars. Data are presented as the mean ±SD, $^{**}P < 0.01$. (*C*) RNA-seq-based gene expression values (FPKM) of *Cdyl* and *Cdyl2* in XY gonadal somatic cells at E11.5 (SRA: PRJNA557299) (10). Data are presented as the mean ±SD (n = 3).

to gene regulation in male gonadal sex determination. We purified *Nr5a1*-expressing gonadal somatic cells from E11.5 XY *Cdyl*$^{\Delta/\Delta}$ embryos according to a previously developed method (5, 24) and then analyzed their mRNA expression (Dataset S1). Notably, the number of *Nr5a1*-expressing gonadal somatic cells was indistinguishable between the XY *Cdyl*$^{\Delta/\Delta}$ and XY *Cdyl*$^{\Delta/+}$ gonads (*SI Appendix*, Fig. S3*A*), suggesting that *Cdyl* deficiency may not influence the growth potential of gonadal somatic cells until E11.5. We found that 1,394 genes showed decreased expression and 215 genes showed increased expression in XY *Cdyl*$^{\Delta/\Delta}$ gonadal somatic cells compared with those in XY *Cdyl*$^{\Delta/+}$ gonadal somatic cells (fold change > |1.3|, *P*-value < 0.05). Genes the expression of which was increased in XY *Cdyl*$^{\Delta/\Delta}$ gonadal somatic cells contained *Gadd45g* and *Emx2*, which are involved in gonadogeneisis and *Sry* regulation (Fig. 3 *A* and *B*). Genes the expression of which was decreased in XY *Cdyl*$^{\Delta/\Delta}$ gonadal somatic cells contained a set of testis-promoting genes, including *Sox9* (Fig. 3 *A*–*D*). Intriguingly, neither the expression of *Sry* nor the expression of genes known to be involved in *Sry* regulation was compromised in XY *Cdyl*$^{\Delta/\Delta}$ gonadal somatic cells (Fig. 3 *A*–*C*), indicating that CDYL regulates *Sox9* expression without influencing *Sry* expression. Consistent with the reduced expression of *Sox9*, expression of the downstream target genes of SOX9, such as *Fgf9*, was also reduced (25) (Fig. 3 *A* and *D*).

To address the mode of action of CDYL in male gonadal sex determination in more detail, we examined the protein expression of SRY and SOX9 in E11.5 gonads by immunofluorescence (Fig. 3 *E* and *F*). Simultaneous staining of gonadal somatic cells with an anti-GATA4 antibody indicated that the number of GATA4+ cells was indistinguishable between XY *Cdyl*$^{\Delta/\Delta}$ and XY *Cdyl*$^{\Delta/+}$ gonads, further supporting the notion that CDYL did not influence the growth potential of gonadal somatic cells. The ratio of SRY+ cells to GATA4+ cells was also similar between XY *Cdyl*$^{\Delta/\Delta}$ and XY *Cdyl*$^{\Delta/+}$ gonads. Furthermore, the signal intensity for SRY was

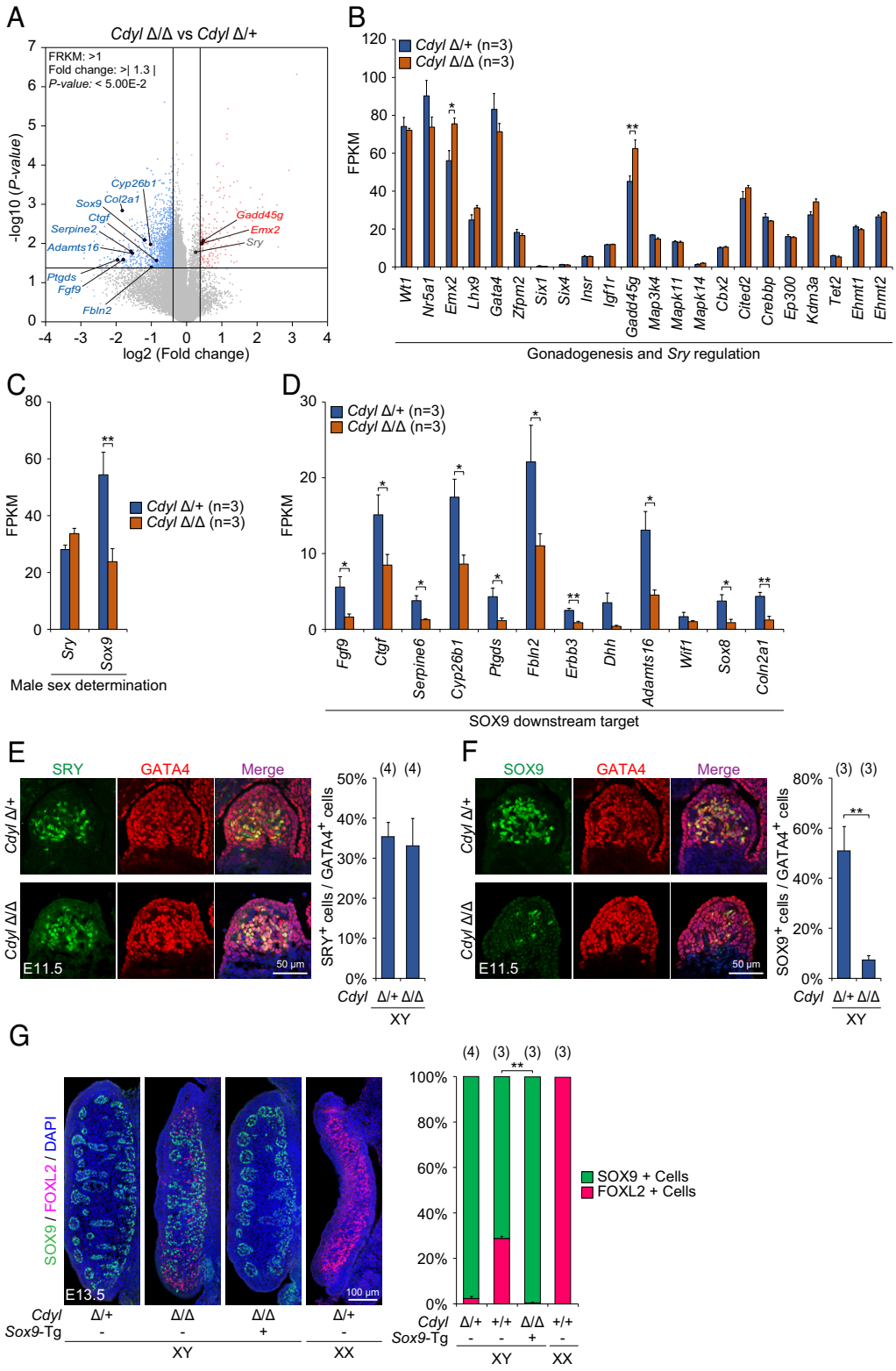

Fig. 3. *Cdyl* deficiency reduces *Sox9* expression without affecting *Sry* expression. (*A*) Gonadal somatic cells were purified from of E11.5 XY *Cdyl*$^{\Delta/+}$ and *Cdyl*$^{\Delta/\Delta}$ embryos and then subjected to poly(A)$^{+}$ RNA-seq analysis. FPKM values of 11,636 genes (FPKM > 1) were plotted in a volcano plot. The *x* axis and *y* axis display the log2 FC-value and the significance represented with log10 *P* value, respectively. Red and blue dots represent upregulated (FC > 1.3, $P < 0.05$) and downregulated genes (FC > 1.3, $P < 0.05$), respectively, in XY *Cdyl*$^{\Delta/\Delta}$ gonadal somatic cells compared to those in XY *Cdyl*$^{\Delta/+}$ control gonadal somatic cells. Genes shown in blue represent *Sox9* and its downstream target genes. (*B–D*) Comparison of expression values (FPKM) of the genes involved in the testis-promoting pathway between E11.5 XY *Cdyl*$^{\Delta/+}$ and *Cdyl*$^{\Delta/\Delta}$ gonadal somatic cells. (*B*) Expression values of the genes involved in gonadogeneisis and/or *Sry* regulation. (*C*) Expression values of male gonad sex-determining genes *Sry* and *Sox9*. (*D*) Expression values of SOX9 downstream target genes. Data are presented as the mean ±SD (n = 3), $^{*}P < 0.05$. $^{**}P < 0.01$. (*E* and *F*) Co-immunostaining profiles for SRY (green) and GATA4 (red) (*E*), or SOX9 (green) and GATA4 (red) (*F*) in the central regions of E11.5 XY *Cdyl*$^{\Delta/+}$ and *Cdyl*$^{\Delta/\Delta}$ gonads. The ratios of SRY+ (*E*), or SOX9+ (*F*) to GATA4+ cells are summarized on the *Right*. The number of examined embryos is shown above the bars. Data are presented as the mean ±SD. $^{**}P < 0.01$. (*G*) Evaluation of gonadal sex differentiation of XY *Cdyl*$^{\Delta/\Delta}$ and *Wt1-Sox9*+; *Cdyl*$^{\Delta/\Delta}$ embryos by immunofluorescence. E13.5 gonads of the indicated genotypes were co-stained with antibodies against SOX9 and FOXL2. The ratio of SOX9+ to FOXL2+ cells is summarized on the *Right*. The green and red bars indicate SOX9+ and FOXL2+ cells, respectively. The number of embryos examined is shown above the bars. Data are presented as the mean ±SD, $^{**}P < 0.01$.

comparable between XY *Cdyl*$^{\Delta/\Delta}$ and XY *Cdyl*$^{\Delta/+}$ gonads (Fig. 3*E*). These results excluded the possibility that CDYL might regulate SRY expression post-transcriptionally. In contrast, *Cdyl* deficiency led to dramatic reduction in SOX9+ cells in E11.5 embryonic gonads; the ratio of SOX9+ cells to GATA4+ cells in XY *Cdyl*$^{\Delta/\Delta}$ gonads was only 10% of that in XY *Cdyl*$^{\Delta/+}$ gonads (Fig. 3*F*). These data confirmed that CDYL regulates *Sox9* expression but not *Sry* expression.

Based on the results described above, we speculated that reduced expression of *Sox9* might be the cause of perturbed male gonadal sex development in XY *Cdyl*$^{\Delta/\Delta}$ mice. To evaluate this possibility, we examined whether experimentally restoring *Sox9* function could rescue the mutant phenotype of XY *Cdyl*$^{\Delta/\Delta}$ mice. A previous study showed that *Wt1-Sox9* transgene (*Wt1-Sox9*) activates the testis-promoting pathway in XX embryos (26). By sequentially crossing the *Wt1-Sox9* allele with the *Cdyl*$^{\Delta}$ background, we generated XY *Wt1-Sox9*+; *Cdyl*$^{\Delta/\Delta}$ embryos and examined their gonadal sex development. We found that *Wt1-Sox9* transgene clearly rescued the ovotestis phenotype of XY *Cdyl*$^{\Delta/\Delta}$ gonads at E13.5 (Fig. 3*G*). Thus, we concluded that reduced expression of *Sox9* is in fact the cause of perturbed male gonadal sex development in XY *Cdyl*$^{\Delta/\Delta}$ embryos.

CDYL Positively Regulates SOX9 Expression by Suppressing the Ovary-Promoting Gene *Wnt4*. CDYL is involved in the transcriptional co-repressor complex (27). Accordingly, canonical CDYL target genes *Scn8a*, *Rims2,* and *Chrm4* were derepressed in *Cdyl*-deficient gonadal somatic cells (20) (Fig. 4 *A* and *B*). Thus, we presumed that CDYL might indirectly enhance *Sox9* expression by suppressing the repressor(s) of *Sox9*. Previous studies have demonstrated that ovary-promoting genes *Rspo1*, *Wnt4*, *Ctnnb1*, *Foxl2*, *Esr1/2,* and *Lats1/2* repress *Sox9* (28–30). Among these genes, *Wnt4* expression was upregulated in E11.5 XY *Cdyl*$^{\Delta/\Delta}$ gonadal somatic cells approximately 1.3-fold compared to *Cdyl*$^{\Delta/+}$ gonadal somatic cells (Fig. 4 *A* and *C*). Consistent with this result, WNT4 downstream genes *Nr0b1*, *Bmp2*, *Fst,* and *Lef1* (31–33) were upregulated in these cells (Fig. 4 *A* and *D*). The expression of other transcriptional repressors of *Sox9*, such as *Rspo1*, was either unchanged or undetectable in these gonads (Fig. 4 *A* and *C*).

We found that *Wnt4* expression was already derepressed prior to *Sry*/*Sox9* activation in E10.5 XY *Cdyl*$^{\Delta/\Delta}$ gonads (Fig. 4*E*), indicating that *Wnt4* derepression is not a consequence of the failed activation of male gonadal sex determination but might intrinsically come from *Cdyl* deficiency. To further evaluate the cause-and-effect relationship between upregulation of *Wnt4* and downregulation of *Sox9* in XY *Cdyl*$^{\Delta/\Delta}$ gonads, we examined whether a reduced gene dosage of *Wnt4* might restore SOX9 expression in XY *Cdyl*$^{\Delta/\Delta}$ embryonic gonads. We generated a mutant allele of *Wnt4* (*Wnt4*$^{\Delta}$) using the CRISPR/Cas9 system (*SI Appendix*, Fig. S4*A*), which was designed to produce a mutant WNT4 protein lacking the receptor-binding site (34). By sequentially crossing the *Wnt4*$^{\Delta}$ allele with the *Cdyl*$^{\Delta}$ background, we obtained XY *Wnt4*$^{\Delta/+}$; *Cdyl*$^{\Delta/\Delta}$ embryos and examined their sex development (Fig. 4*F*). We found that the number of SOX9+ cells was significantly higher in E11.5 gonads of XY *Wnt4*$^{\Delta/+}$; *Cdyl*$^{\Delta/\Delta}$ embryos than that in XY *Wnt4*$^{+/+}$; *Cdyl*$^{\Delta/\Delta}$ littermates. We also found that the ratio of SOX9+ cells to the sum of SOX9+ and FOXL2+ cells in E13.5 gonads was significantly higher in XY *Wnt4*$^{\Delta/+}$; *Cdyl*$^{\Delta/\Delta}$ embryos (>90%) than that in XY *Wnt4*$^{+/+}$; *Cdyl*$^{\Delta/\Delta}$ littermates (~60%) (*SI Appendix*, Fig. S4*B*). These data support that downregulation of *Sox9* in XY *Cdyl*$^{\Delta/\Delta}$ gonads might be a consequence of upregulation of *Wnt4*.

We next evaluated whether CDYL directly targets the *Wnt4* locus in gonadal somatic cells during male gonadal sex determination. As we could not detect endogenously expressed CDYL using commercially available antibodies, we established a mouse line carrying a modified *Cdyl* allele (*Cdyl*^{3xTY1}), which was designed to produce the CDYL protein with a carboxy-terminal triple TY1 tag (3xTY1) (*SI Appendix*, Fig. S4*C*). Western blot analysis using purified *Nr5a1*-expressing gonadal somatic cells indicated that CDYL-3xTY1 was expressed in E11.5 XY *Cdyl*$^{3xTY1/3xTY1}$ gonadal somatic cells (*SI Appendix*, Fig. S4*C*). We further investigated protein expression of CDYL-3xTY1 in the developing gonads by immunofluorescence. CDYL-3xTY1 was expressed in the nuclei of GATA4+ gonadal somatic cells of XY *Cdyl*$^{3xTY1/3xTY1}$ embryos at E11.5 (*SI Appendix*, Fig. S4*C*). Notably, CDYL-3xTY1 expressed more strongly in primordial germ cells than in gonadal somatic cells.

Recently, Mayère et al. identified a novel population of supporting-like cells (SLCs) in the developing mouse gonads by using single-cell (sc) RNA-seq analysis (35). They showed that *Wnt4* expression in E11.5 XY SLCs was higher than in E11.5 XY Sertoli cells and decreases as development progresses (35) (*SI Appendix*, Fig. S4*D*). We investigated the relationship between *Cdyl* and *Wnt4* expression by using their scRNA-seq data set (GEO: GSE184708). Interestingly, *Cdyl* expression was higher in E11.5 XY Sertoli cells than in E11.5 XY SLCs and increased in both cells with development (*SI Appendix*, Fig. S4*D*). Furthermore, *Cdyl* expression was higher in XY Sertoli cells than in XX pre-granulosa cells, and *Cdyl* and *Wnt4* expression were inversely correlated (*SI Appendix*, Fig. S4*D*). These results raise a possibility that CDYL may be involved in the regulation of *Wnt4* in various cells during gonad development.

To determine the target loci of CDYL, we purified gonadal somatic cells from E11.5 XY *Cdyl*$^{3xTY1/3xTY1}$ gonads and then subjected them to chromatin immunoprecipitation (ChIP) analysis (Fig. 4*G* and *SI Appendix*, Fig. S4*E*). We found that CDYL-3xTY1 is specifically enriched in the canonical CDYL target gene loci in *Cdyl* $^{3xTY1/3xTY1}$ gonadal somatic cells (*SI Appendix*, Fig. S4*E*), indicating that this ChIP method was effective in determining CDYL target genes. Importantly, CDYL-3xTY1 is enriched in the *Wnt4* promoter region, but neither in the region distal to the *Wnt4* promoter nor in the promoter region of CBX2 target gene *Lef1* (Fig. 4*G* and *SI Appendix*, Fig. S4*E*), indicating that CDYL directly and selectively targets the *Wnt4* promoter in gonadal somatic cells during male sex determination.

Finally, we evaluated how CDYL deficiency influences the epigenetic state of the *Wnt4* locus in gonadal somatic cells. ChIP analysis demonstrated that H3K27me3, but not H3K9me2, was decreased in the *Wnt4* promoter in *Cdyl*-deficient gonadal somatic cells at E11.5 (Fig. 4*H* and *SI Appendix*, Fig. S4*F*), indicating that CDYL suppresses *Wnt4* by maintaining its H3K27me3 levels. A previous study demonstrated that CDYL interacts with the H3K27 tri-methyltransferase EZH2 (19); therefore, we proposed a model in which CDYL repress *Wnt4* transcription by tethering EZH2 to its promoter (Fig. 4*I*). CDYL deficiency led to the failure of EZH2-mediated H3K27 tri-methylation at the *Wnt4* promoter, thereby inducing its derepression. Derepressed *Wnt4* led to the repression of *Sox9* transcription.

Discussion

Recent findings on mammalian sex development suggest that the fate decision of sexually undifferentiated gonads depends not only on transcriptional activation of *Sry*, but also on a delicate expression balance between the testis- and ovary-promoting genes (36). We previously showed that several epigenetic writer and eraser proteins substantially contribute to the fine-tuning of *Sry* expression (37). Here we showed that an epigenetic reader protein CDYL reinforces male gonadal sex determination by tilting the expression balance between the testis- and ovary-promoting genes.

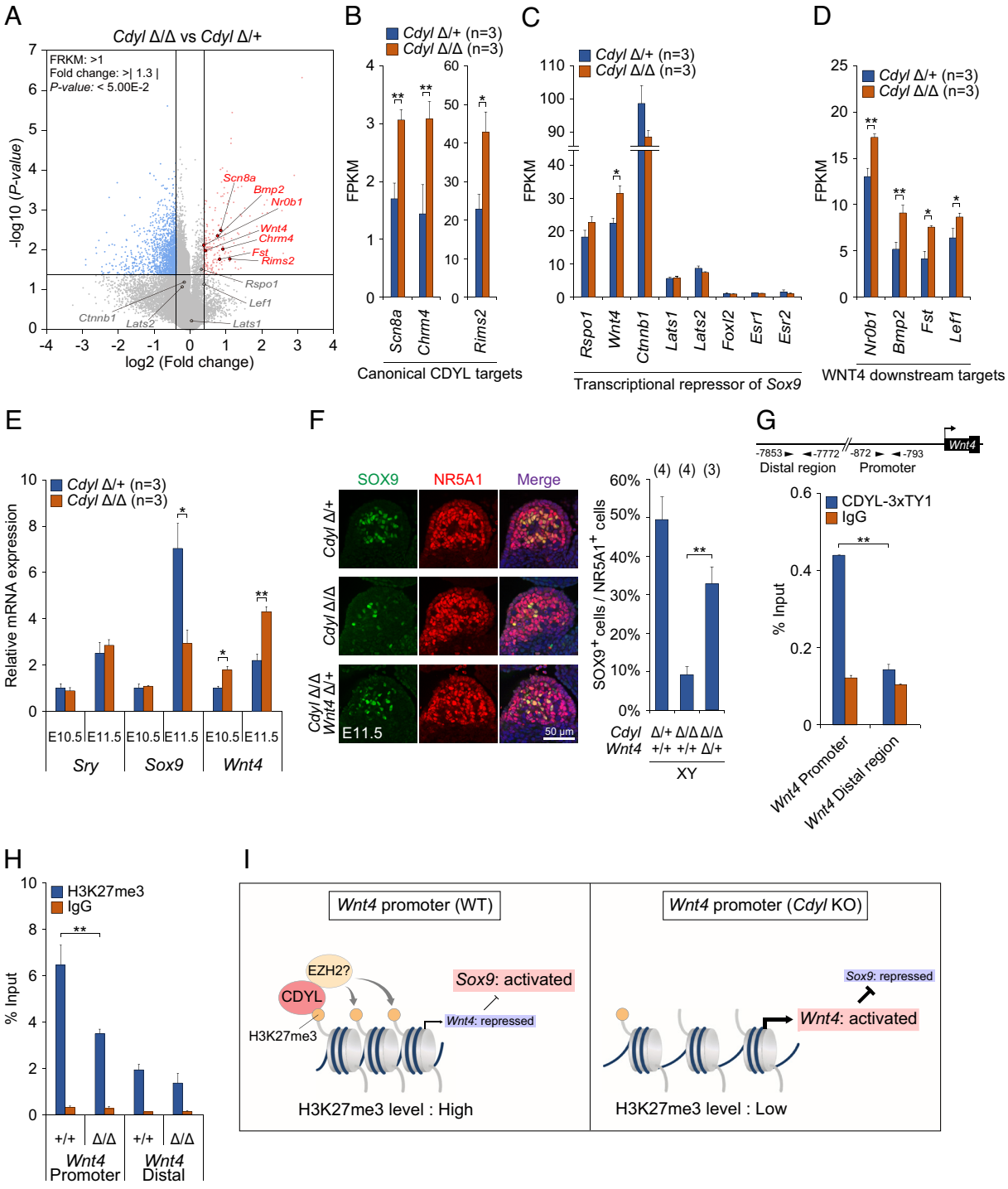

Fig. 4. CDYL positively regulates SOX9 expression through suppressing ovary-promoting gene, *Wnt4*. (*A*) Typically upregulated genes are highlighted in the volcano plot showing gene expression profiles of E11.5 XY *Cdyl*$^{\Delta/+}$ and *Cdyl*$^{\Delta/\Delta}$ gonadal somatic cells. Canonical CDYL target genes *Scn8a*, *Chrm4* and *Rims2* were upregulated by *Cdyl* deficiency. *Wnt4* and its downstream target genes *Nr0b1*, *Bmp2*, *Fst* and *Lef1* were also upregulated by *Cdyl* deficiency. (*B–D*) Comparison of gene expression values (FPKM) between E11.5 XY *Cdyl*$^{\Delta/+}$ and *Cdyl*$^{\Delta/\Delta}$ gonadal somatic cells. (*B*) Expression values of the canonical CDYL target genes. (*C*) Expression values of the known transcriptional repressors for *Sox9*. (*D*) Expression values of *Wnt4* downstream target genes. Data are presented as the mean ±SD (n = 3), *P < 0.05. **P < 0.01. (*E*) Expression kinetics of *Sry*, *Sox9* and *Wnt4* in XY *Cdyl*$^{\Delta/+}$ and *Cdyl*$^{\Delta/\Delta}$ gonads. Gonadal somatic cells were purified from E10.5 and E11.5 embryos and subjected to quantitative RT-qPCR analysis. mRNA expression levels in E10.5 XY *Cdyl*$^{\Delta/+}$ gonadal somatic cells were defined as 1. The number of embryos examined is shown above the bars. Data are presented as the mean ±SD (n = 3), *P < 0.05, **P < 0.01. (*F*) Co-immunostaining profiles of SOX9 (green) and NR5A1 (red) in the central regions of E11.5 XY gonads of the indicated genotypes. NR5A1+ cells represent gonadal somatic cells. The ratio of SOX9+ to NR5A1+ cells is summarized on the *Right*. The number of examined embryos is shown above the bars. Data are presented as the mean ±SD, **P < 0.01. (*G*) Evaluation of CDYL-3xTY1 enrichment in the *Wnt4* promoter in E11.5 gonadal somatic cells. E11.5 gonadal somatic cells were purified from XY *Cdyl*$^{3xTY1/3xTY1}$ embryos and then subjected to ChIP-qPCR analysis using anti-TY1 antibody. IgG indicates negative control. Primer locations are shown at the *Top*. *Wnt4* distal region represents a control locus with low levels of H3K27me3 in gonadal somatic cells (9). The ChIP experiment was performed independently twice with similar results. Data are presented as the mean ±SD. **P < 0.01. (*H*) ChIP-qPCR analyses for H3K27me3 at the *Wnt4* promoter and in E11.5 XY *Cdyl*$^{+/+}$ and *Cdyl*$^{\Delta/\Delta}$ gonadal somatic cells. IgG indicates negative control. The ChIP experiment was performed independently three times with similar results. Data are presented as the mean ±SD, **P < 0.01. (*I*) Role of CDYL in the testis-promoting pathway. CDYL represses *Wnt4* transcription through tethering H3K27 methyltransferase to its promoter. CDYL deficiency leads to the failure of H3K27 methylation at the *Wnt4* promoter, which induces *Wnt4* derepression and subsequent *Sox9* repression.

CDYL is a reader protein of H3K9me2/3 and H3K27me3 (14). Based on the fact that CDYL interacts with the H3K9 methyltransferase, GLP/G9a (15, 16), which is the responsible enzyme for H3K9me2 at the *Sry* locus (6), we initially predicted that CDYL might negatively regulate male gonadal development by repressing *Sry*. However, genetic evaluation using a *Jmjd1a*-deficient background indicated that CDYL is a positive regulator of male gonadal development. CDYL indirectly activated the testis-promoting gene *Sox9* by directly repressing the ovary-promoting gene *Wnt4*. A decrease in H3K27me3, but not H3K9me2, was prominent in the *Wnt4* promoter in XY *Cdyl*-deficient gonadal somatic cells; thus, it seems likely that CDYL represses *Wnt4* by maintaining the H3K27me3 levels of the *Wnt4* promoter. It is also known that CDYL represses *Bdnf*, which is a key player in promoting dendrite development in rat and mouse hippocampal neurons (19). In this case, CDYL interacts with the H3K27 methyltransferase EZH2 and recruits its methyltransferase activity to the *Bdnf* promoter. Collectively, it is plausible that CDYL can recruit different histone modification enzymes in a locus-dependent and cell type-dependent manner.

Although *Sox9* expression was significantly reduced in XY *Cdyl*-deficient embryonic gonads, only a subpopulation (~10%) of XY *Cdyl*-deficient mice exhibited sex reversal. A previous study predicted that the threshold level of *Sox9* expression required for testis development in mice is approximately 25% of that of wild-type (38). We found that *Sox9* expression in XY *Cdyl*-deficient gonads at E11.5 was reduced to approximately 40% of that in XY control gonads (Fig. 3*C*). Thus, we speculate that *Sox9* expression in XY *Cdyl*-deficient embryonic gonads is still higher than the threshold, which may account for the partial sex-reversal phenotype of XY *Cdyl*-deficient mice.

CBX2 is a subunit of canonical polycomb repressive complex 1, which acts as a reader protein for H3K27me3 and mediates chromatin compaction. *Cbx2*-deficient mice exhibit failed *Sry* activation and XY sex-reversal phenotype (8). Garcia-Moreno et al. demonstrated that CBX2 stabilized the testis-promoting pathway by directly binding to a WNT signal downstream target gene *Lef1* (9). In XY gonads lacking CBX2, *Lef1* was derepressed, which might cause repression of *Sry*. Our current study demonstrated that CDYL is another reader protein that stabilizes the testis-promoting pathway. However, intriguingly, our results suggest that *Wnt4* is a direct target of CDYL but *Lef1* may not (*SI Appendix*, Fig. S4*E*). We therefore propose that the points of action of CBX2 and CDYL during male gonad development seem to be distinct: CBX2 reinforces *Sry* expression by repressing *Lef1*, whereas CDYL reinforces *Sox9* expression by repressing *Wnt4*. The next important step is to clarify the molecular mechanism by which CBX2 and CDYL selectively recognize their target loci. Previous studies indicate that the chromodomains of CDYL family proteins and CBX family proteins exhibit different binding preferences for methylated histone H3 (39, 40), which may explain the difference in target genes between CDYL and CBX2.

Previous studies have demonstrated that the histone demethylase JMJD1A and the histone acetyltransferases CBP/p300 play a pivotal role in mouse *Sry* activation (5, 7). In addition to these erasers and writers, our current study highlights the importance of reader proteins in male gonadal sex determination. The mammalian genome encodes many types of reader proteins that positively or negatively regulate transcription (2). We found that a number of these genes were expressed in E11.5 gonadal somatic cells (41); therefore, it is plausible that a variety of reader proteins might contribute to gene regulation in mammalian gonadal sex development.

Materials and Methods

Animals. All animal experiments were approved and performed in accordance with the relevant guidelines and regulations of the Animal Care Committee of Osaka University (FBS-18-014). Mice were housed under a 12/12 h light/dark cycle at 22 to 24 °C, with a humidity of approximately 50%. Mice (C57BL/6J and ICR) were supplied by SLC (Shimizu Laboratory Supplier, Kyoto) in Japan. Mouse lines were sequentially backcrossed with C57BL/6J mice, and F5 or later generations were used. In the experiments shown in Figs. 2 *A* and *B* and 4*F* and *SI Appendix*, Figs. S2 *B* and *C* and S4*B*, we used mice with a CBA-derived Y chromosome in combination with B6-derived autosomes (5). Embryos were staged by counting tail somites as previously described, where 6 to 8 ts and 15 to 18 ts correspond to approximately E10.5 and E11.5, respectively.

Generation of the Mutant Mice using a CRISPR/Cas9 System. Mutant mice were produced by electroporating Cas9 protein, guide RNA (gRNA), and ssODNs into mouse zygotes according to a recently published protocol (42). Briefly, 50 ng/μL Cas9 protein and 100 ng/μL each gRNAs targeting *Cdyl, Cdyl2,* and *Wnt4* (shown in *SI Appendix*, Figs. S1 *A* and *B* and S4*A*) were introduced into zygotes (C57BL/6J × C57BL/6J) by electroporation using Genome Editor GEB15 (BEX, Tokyo, Japan). When we knocked in the epitope tags to endogenous *Cdyl*, we added an additional 500 ng/μL ssODN (shown in *SI Appendix*, Fig. S4*C*). The electroporation conditions were 30 V (3 ms ON + 97 ms OFF) × 4 cycles. The surviving 2-cell-stage embryos were transferred to the oviducts of pseudopregnant females (ICR). The mutant mice were backcrossed for more than three generations into a C57BL6/J background.

Isolation of Gonadal Somatic Cells by MACS. MACS was performed as previously described (5). Briefly, a single-cell suspension was prepared by trypsinizing the gonads and mesonephros isolated from embryos carrying the *Nr5a1/CD271*-transgene. Immunomagnetic isolation of CD271-expressing cells was performed according to the standard protocol (Miltenyi Biotech).

RNA Expression Analysis. Total RNA from hCD271-positive cells and a pair of gonads/mesonephros was extracted using TRIzol (Invitrogen). The ReverTra Ace qPCR RT Kit (TOYOBO) was used for cDNA synthesis, following the manufacturer's instructions. Subsequently, cDNA was used as a template for RT-qPCR using a StepOnePlus Real-Time PCR System (Applied Biosystems) and SYBR Premix Ex Taq II (TaKaRa) with gene-specific primers. The primer sets used in this analysis were as follows.

Sry forward 5′-TACCTACTTACTAACAGCTGACATCAC-3′
Sry reverse 5′-TGTCATGAGACTGCCAACCACAGGG-3′
Sox9 forward 5′-AGGAAGCTGGCAGACCAGTA-3′
Sox9 reverse 5′-CGTTCTTCACCGACTTCCTC-3′
Wnt4 forward 5′-TGTCCAGCTCCAAACTGTCTC-3′
Wnt4 reverse 5′-GAAGTGGACCTTCTGGACAGC-3′
GAPDH forward 5′-ATGAATACGGCTACAGCAACAGG-3′
GAPDH reverse 5′-CTCTTGCTCAGTGTCCTTGCTG-3′

RNA-Seq Analysis. RNA-seq shown in Fig. 2*C* was performed as previously described (10). RNA sequencing data have been uploaded to NCBI Sequence Read Archive (SRA) with the accession number PRJNA557299. For single-cell RNA-seq analysis in *SI Appendix*, Fig. S4*D*, raw counts data were obtained from NCBI Gene Expression Omnibus (GEO: GSE184708) (35). The data were log2-normalized and clustered using Seurat R package (version 4.1.0) (43). The data were separated into 50 clusters, and cell type of each cluster was inferred by its gene expression patterns. The mean of normalized count in each cell type was used for the analysis. RNA-seq for *SI Appendix*, Figs. S3*A* and S4*A* was performed as follows. Total RNA from hCD271-positive cells was extracted using the Direct-zol RNA MicroPrep kit (Zymo Research). Quality control checks for length distribution and concentration of RNA fragments in the prepared libraries were performed using the Agilent 2100 Bioanalyzer (Agilent Technologies). The libraries of the samples were prepared using the SMARTer® Stranded Total RNA-Seq Kit v2 - Pico Input Mammalian (TaKaRa). The samples were sequenced as paired-end, 150 base-length reads on an Illumina NovaSeq 6000 instrument (Illumina Inc.) with 30 million reads. Raw sequence reads were mapped to mm10 using STAR aligner. Fragments per kilobase of exon per million reads mapped (FPKM) were calculated with an in-house Perl script at K.K. DNAFORM using raw counts obtained with

featureCounts (v1.6.4) (a software program in the Subread package). The FPKM values are listed in Dataset S1. The accession number for the RNA-seq data generated in this study is GEO: GSE226049.

Western Blotting Analysis. Western blotting was performed as previously described (44, 45). Briefly, cells were lysed by boiling in SDS sample buffer. Before the lysed proteins were applied to polyacrylamide-SDS gels, 2-mercaptoethanol was added to denature the proteins. The lysed proteins were separated on polyacrylamide-SDS gels and blotted onto nitrocellulose membranes. Non-specific protein binding was blocked with 5% skim milk/TBST (Tris-buffered saline with Tween 20), and the membranes were probed using a rabbit anti-TY1 (GeneScript, A01004) with Signal Enhancer HIKARI (Nacalai Tesque). The membranes were then incubated with HRP-conjugated antibodies against rabbit IgG in 5% skim milk/TBST. Detection was performed using Western Lightning Plus ECL (PerkinElmer).

Immunohistochemical Staining. Immunohistochemical staining was performed as previously described (10). Briefly, tissues were fixed in 4% paraformaldehyde, embedded in Tissue-Tek OTC compound (Sakura Finetek, Japan), and cut into 10-μm sections. The sections were incubated with primary antibodies (goat anti-GATA4 (Santa Cruz, sc-1237), rat anti-NR5A1 (TransGenic, KO610), guinea pig anti-SRY (6), rabbit anti-SOX9 (Millipore, AB5535), goat anti-FOXL2 (Abcam, ab-5096) and rabbit anti-TY1 (GeneScript, A01004)), overnight at 4 °C. For fluorescence staining, sections were incubated with Alexa-conjugated secondary antibodies (Life Technologies) at room temperature for 1 h and counterstained with DAPI. The sections were mounted in Vectashield (Vector) and observed under a confocal laser-scanning microscope (LSM700, Carl Zeiss).

ChIP Analysis. Gonadal somatic cells were purified from embryos using MACS. Cross-link ChIP analysis of H3K9me2, HeK27me3, and CDYL-3xTY1 purified gonadal somatic cells from multiple embryos (histone modifications; 3 to 4 embryos, CDYL-3xTY1; >20 embryos) wAS pooled and then cross-linked with 25 mM DSG (Thermo Fisher Scientific) and 1% formaldehyde, and subjected to ChIP analysis with mouse anti-H3K9me2 (abcam, ab1220), mouse anti-H3K27me3 (Millipore, 07-449) and mixed rabbit anti-TY1 (GeneScript, A01004)/mouse anti-TY1 (diagenode, C15200054) following a protocol described previously (5). The primer sets used in this analysis were as follows.

Wnt4 promoter forward 5′-GTGCCAGACACCAAGCTAAGG-3′
Wnt4 promoter reverse 5′-GTCTGCTTGGGTTTCTGTTCG-3′
Wnt4 distal region forward 5′-AGCGTACAGGCTTCTGGAATG-3′
Wnt4 distal region reverse 5′-TGATGCCTTGAAACTGTGGTG-3′
Lef1 promoter forward 5′-CTACAGATGGCTGCCTCACTG-3′
Lef1 promoter reverse 5′-GGGGCTTAAGTTTGGAAACAC-3′
Sry promoter forward 5′-TGGTCAGTGGCTTTTAGCTCT-3′
Sry promoter reverse 5′-AGATGTGATGCAAAGAGAAACA-3′
Scn8a forward 5′-ATGTGGTGGGTTTTGTGTAGC-3′
Scn8a reverse 5′-ACCTCAAATGAAAACCGAAGG-3′
Rims2 forward 5′-GTCAGCCCATTCACACTCCT-3′
Rims2 reverse 5′-TCGTCTCCCTGGACAAGACA-3′
Chrm4 forward 5′-CAGCCCTTGCAGGAGAGTAG-3′
Chrm4 reverse 5′GAGTACCGGTCACCCACAAA-3′
Major satellite forward 5′-GACGACTTGAAAAATGACGAAATC-3′
Major satellite reverse 5′-CATATTCCAGGTCCTTCAGTGTGC-3′
Actb promoter forward 5′-GCGTGTCCCTCAAACAAGAG-3′
Actb promoter reverse 5′-TGTCACGTGGATATCGAGCAC-3′
GAPDH promoter forward 5′-CTCCCTGCCTTTTAAGCAAAG-3′
GAPDH promoter reverse 5′-TAGGCCAGTGCAACATGAAAC-3′

Data, Materials, and Software Availability. RNA-seq data have been deposited in NCBI SRA (PRJNA557299) (10) and NCBI GEO database (GSE184708) (35). RNA-seq data in this study are deposited in NCBI GEO database (GSE226049) (46). All other study data are included in the article and/or supporting information.

ACKNOWLEDGMENTS. We are grateful to the members of the Tachibana Laboratory for their technical support and stimulating discussions. We thank K. Morohashi and A. Schedl for *Wt1-Sox9* transgenic mice. This study was supported by JSPS KAKENHI [grant numbers 16K18429 (N.O.), 21K15067 (R.M.), 17H06424 (M.T.), and 21H04769 (M.T.)].

1. K. Hyun *et al.*, Writing, erasing and reading histone lysine methylations. *Exp. Mol. Med.* **49**, e324 (2017).
2. S. D. Taverna *et al.*, How chromatin-binding modules interpret histone modifications: Lessons from professional pocket pickers. *Nat. Struct. Mol. Biol.* **14**, 1025–1040 (2007).
3. N. Gonen *et al.*, Sex reversal following deletion of a single distal enhancer of *Sox9*. *Science* **360**, 1469–1473 (2018).
4. M. García-Acero *et al.*, Disorders of sexual development: Current status and progress in the diagnostic approach. *Curr. Urol.* **13**, 169–178 (2019).
5. S. Kuroki *et al.*, Epigenetic regulation of mouse sex determination by the histone demethylase Jmjd1a. *Science* **341**, 1106–1109 (2013).
6. S. Kuroki *et al.*, Rescuing the aberrant sex development of H3K9 demethylase Jmjd1a-deficient mice by modulating H3K9 methylation balance. *PLoS Genet.* **13**, e1007034 (2017).
7. G. A. Carre *et al.*, Loss of p300 and CBP disrupts histone acetylation at the mouse Sry promoter and causes XY gonadal sex reversal. *Hum. Mol. Genet.* **27**, 190–198 (2018).
8. Y. Katoh-Fukui *et al.*, Male-to-female sex reversal in M33 mutant mice. *Nature* **393**, 688–692 (1998).
9. S. A. Garcia-Moreno *et al.*, CBX2 is required to stabilize the testis pathway by repressing Wnt signaling. *PLoS Genet.* **15**, e1007895 (2019).
10. N. Okashita *et al.*, TET2 catalyzes active DNA demethylation of the sry promoter and enhances its expression. *Sci. Rep.* **9**, 13462 (2019).
11. B. T. Lahn, D. C. Page, Retroposition of autosomal mRNA yielded testis-specific gene family on human Y chromosome. *Nat. Genet.* **21**, 429–433 (1999).
12. B. T. Lahn *et al.*, Previously uncharacterized histone acetyltransferases implicated in mammalian spermatogenesis. *Proc. Natl. Acad. Sci. U.S.A.* **99**, 8707–8712 (2002).
13. Z. W. Sun *et al.*, Cdyl deficiency brakes neuronal excitability and nociception through promoting Kcnb1 transcription in peripheral sensory neurons. *Adv. Sci. (Weinh.)* **9**, e2104317 (2022).
14. M. Escamilla-Del-Arenal *et al.*, Cdyl, a new partner of the inactive X chromosome and potential reader of H3K27me3 and H3K9me2. *Mol. Cell Biol.* **33**, 5005–5020 (2013).
15. S. C. Sampath *et al.*, Methylation of a histone mimic within the histone methyltransferase G9a regulates protein complex assembly. *Mol. Cell* **27**, 596–608 (2007).
16. L. Fritsch *et al.*, A subset of the histone H3 lysine 9 methyltransferases Suv39h1, G9a, GLP, and SETDB1 participate in a multimeric complex. *Mol. Cell* **37**, 46–56 (2010).
17. Y. Shi *et al.*, Coordinated histone modifications mediated by a CtBP co-repressor complex. *Nature* **422**, 735–738 (2003).
18. P. Mulligan *et al.*, CDYL bridges REST and histone methyltransferases for gene repression and suppression of cellular transformation. *Mol. Cell* **32**, 718–726 (2008).
19. C. Qi *et al.*, Coordinated regulation of dendrite arborization by epigenetic factors CDYL and EZH2. *J. Neurosci.* **34**, 4494–4408 (2014).
20. Y. Liu *et al.*, CDYL suppresses epileptogenesis in mice through repression of axonal Nav1.6 sodium channel expression. *Nat. Commun.* **8**, 355 (2017).
21. L. Wan *et al.*, Generation and neuronal differentiation of induced pluripotent stem cells in Cdyl-/- mice. *Neuroreport* **24**, 114–119 (2013).
22. S. Dorus *et al.*, The CDY-related gene family: Coordinated evolution in copy number, expression profile and protein sequence. *Hum. Mol. Genet.* **12**, 1643–1650 (2003).
23. M. Siouda *et al.*, CDYL2 epigenetically regulates MIR124 to control NF-κB/STAT3-dependent breast cancer cell plasticity. *iScience* **23**, 101141 (2020).
24. S. Kuroki *et al.*, Development of a general-purpose method for cell purification using Cre/loxP-mediated recombination. *Genesis* **53**, 387–393 (2015).
25. Y. Li *et al.*, The sex-determining factors SRY and SOX9 regulate similar target genes and promote testis cord formation during testicular differentiation. *Cell Rep.* **8**, 723–733 (2014).
26. V. P. Vidal *et al.*, Sox9 induces testis development in XX transgenic mice. *Nat. Genet.* **28**, 216–217 (2001).
27. C. Caron *et al.*, Cdyl: A new transcriptional co-repressor. *EMBO Rep.* **4**, 877–882 (2003).
28. D. M. Maatouk *et al.*, Stabilization of beta-catenin in XY gonads causes male-to-female sex-reversal. *Hum. Mol. Genet.* **17**, 2949–2955 (2008).
29. S. Jakob, R. Lovell-Badge, Sex determination and the control of Sox9 expression in mammals. *FEBS J.* **278**, 1002–1009 (2011).
30. M. Tsoi *et al.*, *Lats1* and *Lats2* are required for ovarian granulosa cell fate maintenance. *FASEB J.* **33**, 10819–10832 (2019).
31. H. Mizusaki *et al.*, Dax-1 (dosage-sensitive sex reversal-adrenal hypoplasia congenita critical region on the X chromosome, gene 1) gene transcription is regulated by wnt4 in the female developing gonad. *Mol. Endocrinol.* **17**, 507–519 (2003).
32. H. H. C. Yao *et al.*, Follistatin operates downstream of Wnt4 in mammalian ovary organogenesis. *Dev. Dyn.* **230**, 210–215 (2004).
33. A. A. Chassot *et al.*, Activation of beta-catenin signaling by Rspo1 controls differentiation of the mammalian ovary. *Hum. Mol. Genet.* **17**, 1264–1277 (2008).
34. M. A. Hammad, S. S. Azam, Structural dynamics and inhibitor searching for Wnt-4 protein using comparative computational studies. *Drug Des. Devel. Ther.* **29**, 2449–2461 (2015).
35. C. Mayère *et al.*, Origin, specification and differentiation of a rare supporting-like lineage in the developing mouse gonad. *Sci. Adv.* **8**, eabm0972 (2022).
36. Z. Y. She, W. X. Yang, Molecular mechanisms involved in mammalian primary sex determination. *J. Mol. Endocrinol.* **3**, R21–R37 (2014).
37. N. Okashita, M. Tachibana, Transcriptional regulation of the Y-linked mammalian testis-determining gene SRY. *Sex. Dev.* **15**, 351–359 (2021).
38. N. Gonen *et al.*, Normal levels of Sox9 expression in the developing mouse testis depend on the TES/TESCO enhancer, but this does not act alone. *PLoS Genet.* **13**, e1006520 (2017).
39. W. Fischle *et al.*, Specificity of the chromodomain Y chromosome family of chromodomains for lysine-methylated ARK(S/T) motifs. *J. Biol. Chem.* **283**, 19626–1935 (2008).

40. L. Kaustov *et al.*, Recognition and specificity determinants of the human cbx chromodomains. *J. Biol. Chem.* **286**, 521–529 (2011).
41. I. Stévant *et al.*, Dissecting cell lineage specification and sex fate determination in gonadal somatic cells using single-cell transcriptomics. *Cell Rep.* **26**, 3272–3283 (2019).
42. M. Hashimoto, T. Takemoto, Electroporation enables the efficient mRNA delivery into the mouse zygotes and facilitates CRISPR/Cas9-based genome editing. *Sci. Rep.* **5**, 11315 (2015).
43. Y. Hao *et al.*, Integrated analysis of multimodal single-cell data. *Cell* **184**, 573–3587.e29 (2021).
44. N. Okashita *et al.*, PRDM14 promotes active DNA demethylation through the ten-eleven translocation (TET)-mediated base excision repair pathway in embryonic stem cells. *Development* **141**, 269–280 (2014).
45. R. Maeda, M. Tachibana, HP1 maintains protein stability of H3K9 methyltransferases and demehylases. *EMBO Rep.* **23**, e53581 (2022).
46. N. Okashita, R. Madea, M. Tachibana, Alteration of *gene expression* in E11.5 XY Cdyl deficient gonadal somatic *cells*. *NCBI GEO*. https://www.ncbi.nlm.nih.gov/geo/query/acc.cgi?acc=GSE226049. Deposited 24 February 2023.